Influence of zinc acetate concentration in the preparation of ZnO nanoparticles via chemical bath deposition

F V Molefe[1], **L F Koao**[1], **B F Dejene**[1], **H C Swart**[2]
[1] Department of Physics, University of the Free State (Qwaqwa campus), Private Bag X13 Phuthaditjhaba, 9866, South Africa
[2] Department of Physics, University of the Free State, P.O. Box 339, Bloemfontein, 9300 South Africa

volksfmv@gmail.com

Abstract. Zinc acetate (ZnAc) concentration was varied to prepare ZnO using the chemical bath deposition method (CBD). X-ray diffraction (XRD), scanning electron microscopy (SEM), ultraviolet visible (UV-vis) and photoluminescence (PL) systems were employed to investigate the influence of ZnAc on the structural, morphological, optical and photoluminescence properties. The obtained crystal structure from XRD analysis was the hexagonal wurtzite structure. It was observed that at higher molar concentration of ZnAc the structure changed to mixture of ZnO and ZnAc. The estimated average crystallite size was 23 nm. There was no effect on the crystallite size as ZnAc concentration was varied. SEM images shows non-uniform agglomerated flower like structures at lower concentrations, at the highest ZnAc concentration flowerlike structures are observed to grow into platelets-like structure. There was no effect on the absorption edges and the energy band gap as ZnAc concentration increases in the UV-vis measurements. PL measurements revealed a slight red-shift in the visible region with an increase in ZnAc concentration.

1. Introduction

Zinc oxide (ZnO) is a metal oxide semiconductor material with wide direct band gap energy equal to 3.37 eV [1]. It is an n – type semiconductor which has a moderate high exciton binding energy of 60 meV at room temperature [2]. This large exciton binding energy indicates that efficient excitonic emission in ZnO can persist at room temperature and higher [3]. From the first half of the 20th century ZnO has been under great study even to-date it is still drawing attention due to its unique structure and morphology [4]. This wurtzite n – type semiconductor has potential applications because of various properties that include good transparency, high electron mobility, and strong room temperature luminescence [5]. Simply because ZnO has good optical properties it can be used in solar cells and light emitting devices [6].

Recently nanotechnology is playing a major role in optimizing metal oxide for various applications in the fields such as electronics, material science and optics [7]. Xu *et al* showed that ZnO has different morphologies ranging from the hexagonal shape up to the rhombohedron shape which can be obtained by different methods of preparation [8].

Several techniques have been employed recently to prepare ZnO such as solution combustion method [9]. Three dimensional flower-like morphologies have been synthesized through facile hydrothermal process by Lu *et al* [10] at 95 ^{o}C for 24 hrs who obtained well dispersed flower-like ZnO structures. Koao *et al* [11], reported on the properties of flower-like ZnO nanostructures synthesized using the chemical bath deposition (CBD) technique. They found that by varying the amount of ZnAc there was

no change in morphology and crystal structure, due to high concentration of ZnAc that was used. Following the work of Koao *et al* [11], we prepared ZnO at low ZnAc concentration to study its influence on structural, morphological, optical and luminescence properties using CBD technique. The current study confirms the consistency of CBD method for the formation of flower-like morphology. The CBD method is preferred due to its uses at low temperature and it is relatively inexpensive way of preparation hence it provides a good control of particle size and a uniform morphology.

2. Methodology

The ZnO powders were prepared by the chemical bath deposition method. The following starting materials such as ZnAc ($Zn(O_2CCH_3)_2$), Thiourea ($(NH_2)_2CS$) and Ammonia (25% NH_3) were used. The sample solutions were prepared by dissolving 0.1, 0.12, 0.14, 0.16, 0.18 and 0.2 M of ZnAc in 60 ml of H_2O, respectively, and 0.4 M of ($(NH_2)_2CS$) and also 98.8ml of (25% NH_3), were dissolved into 200 ml of deionized water, respectively. Then a magnetic stirrer was used to stir each of the mixtures for 12 hours at room temperature to ensure homogenous distribution of the solution reagents. An equal volume ratio (1:1:1) was considered for each solution in the following order: 60 ml quantity of ZnAc was first added to the beaker which was placed in the water bath, followed by addition of 60 ml of ($(NH_2)_2CS$) solution while stirring and finally 60 ml of (25% NH_3) solution was also added while continuously stirring. Water bath was maintained to be at a constant desired temperature of 80 ^oC. The white precipitates were then formed within 30 seconds after the solution was placed inside the water bath. The beakers were removed from the bath after 10 minutes. The solution was allowed to stabilize for 12 hours in the lab. Finally the solution was filtered and the dry precipitate was collected, washed several times with 60 ml of ethanol and 60 ml of acetone to remove the residue and desiccated for a maximum of 72 hours to ensure that they are dried prior to characterization. The powders synthesized were characterized by XRD, SEM, UV-vis spectroscopy and PL.

3. Results and discussion

3.1. Structural analysis

Figure 1(a) presents the XRD patterns of ZnO prepared at various concentrations of ZnAc ranging from 0.1 to 0.2 M. All the XRD diffraction peaks observed between 0.1 to 0.18 M match with hexagonal wurtzite structure JCPDS card no. 36-1451, with calculated average lattice constants a = 3.245 Å and c = 5.177 Å. There was no effect on lattice constants as ZnAc concentration increases. At higher ZnAc concentration 0.2 M there is a mixture of ZnO diffraction peaks marked with circles (^{o}) and ZnAc diffraction peaks marked with asterisks (*). The Scherrer's equation [12], was employed to estimate the ZnO mean crystallite size using the full width at half maximum (FWHM) of all the diffraction peaks. The average estimated mean crystallite size of ZnO powders was ~ 23 nm, and there was no change in the crystallite size when increasing ZnAc concentration. From figure 1(b) it is observed that the (101) peak of the ZnO powders have slightly shifted to higher diffraction angles when the ZnAc concentration was increased. The slight shift of the peak position indicates a compaction of the unit cell, simply because Zn^{2+} ions which are in excess prefer to occupy the interstitial sites. Furthermore, the peak shift may be due to increased ZnAc concentrations which help to enhance mobility of atoms, subsequently resulting in improved quality of ZnO crystals [13].

3.2. SEM analysis

The SEM images of the ZnO nanoparticles prepared using the CBD method by varying ZnAc concentration are shown in figure 2(a) – (d). In figure 2(a) the image reveals highly agglomerated flower-like particles for the samples prepared at the low concentration of ZnAc 0.1 M. The image in figure 2(b) shows a slight increase in size of flower-like particles for 0.14 M concentration. From figure 2(c) we have SEM image of sample prepared at 0.18 M, which reveals clearly defined flower-like particles. There are noticeable voids and pores on the surface resulting from the evaporation of water molecules when drying the samples. With increasing the ZnAc concentration to 0.2 M we observed an alteration in the structure wherein small flower-like structures are grown on platelets like structure as shown in figure 2(d). We assume that the observed platelets (big chunks) are caused by the unreacted ZnAc. The possible reason for this type of growth is attributed to higher super-saturation at 0.2 M ZnAc concentration since the atoms are readily available for random growth [14].

When comparing the results presented from figure 2(a) – (c) it can be seen that the morphology is non-uniform flower-like structures, except for the sample prepared at 0.2 M which also showed ZnAc impurities in the XRD spectrum. The origin of different morphology in figure 2(d) is due to aggregation of flower-like particles when unreacted metastable ZnAc undergoes self-hydrolysis [15].

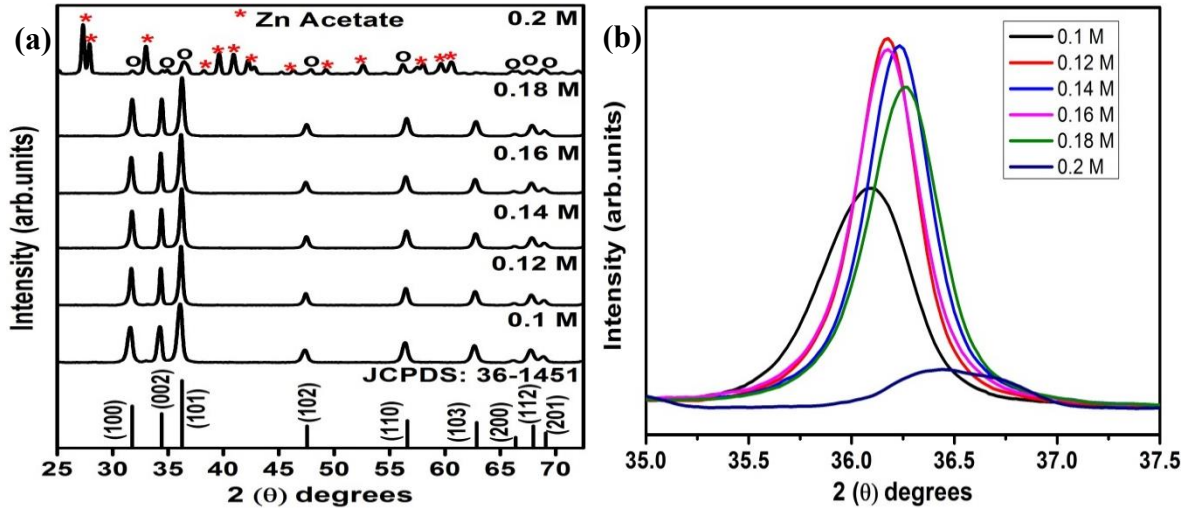

Figure 1. XRD patterns of (a) ZnO nanoparticles prepared at different concentrations of ZnAc using the CBD method as well as the JCPDS standard spectrum, (b) Detail of the (101) peak.

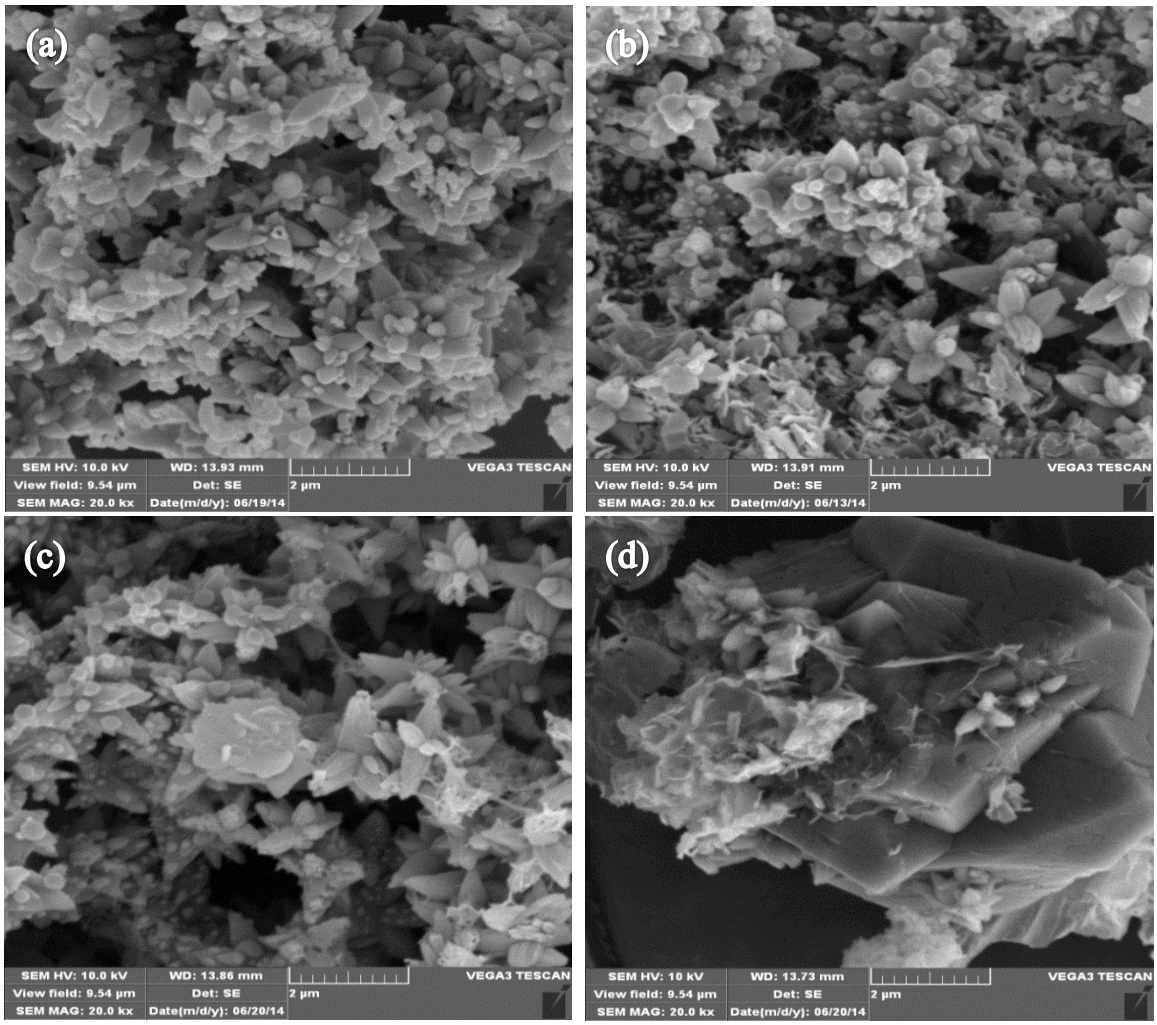

Figure 2. SEM images of ZnO nanoparticles prepared at different concentrations of ZnAc using the CBD method, (a) 0.1 M, (b) 0.14 M, (c) 0.18 M and (d) 0.2 M.

3.3. UV-vis analysis

Figure 3 shows diffuse reflectance measurements of the ZnO nanoparticles in the wavelength range 200 – 800 nm. The percentage reflectance in the visible region increased from ~ 78.5 % at 0.1 M and reached ~ 94.7 % maximum at 0.14 M ZnAc concentration. This indicates that the ZnO absorbs more at low ZnAc concentration. When increasing the ZnAc concentration from 0.1 M to 0.18 M we observed no shift in the absorption band. As illustrated in figure 3 there is a blue shift in absorption band for the sample prepared at 0.2 M ZnAc concentration. This blue shift may be due to ZnAc impurities observed in the XRD spectrum and the formation of platelets like structure observed in the SEM morphology at 0.2 M ZnAc concentration.

The optical band gaps (E_g) for the ZnO powders was calculated from the Kubelka Munk's function $K = (1-R)^2 / 2R$ [16], by extrapolating the linear portion of the graph to $(Khv)^2 = 0$ as shown in figure 4. It is demonstrated in figure 4 that the optical band gaps (E_g) shows no appreciable change for ZnO powders prepared at 0.1 to 0.18 M ZnAc concentrations. The non-change in band gaps can be because of no change in crystallite size when increasing ZnAc concentration. The average estimated energy band gap for ZnO powders prepared at 0.1 to 0.18 M ZnAc concentrations is ~ 3.20 eV. The inset in figure 4 shows the increase in band gap for the sample prepared at 0.2 M ZnAc, which is equal to ~ 4.60 eV. The increase in band gap energy due to increase in the ZnAc to 0.2 M concentration also relates to ZnAc impurities and structural morphology observed in figure 1 and figure 2(d).

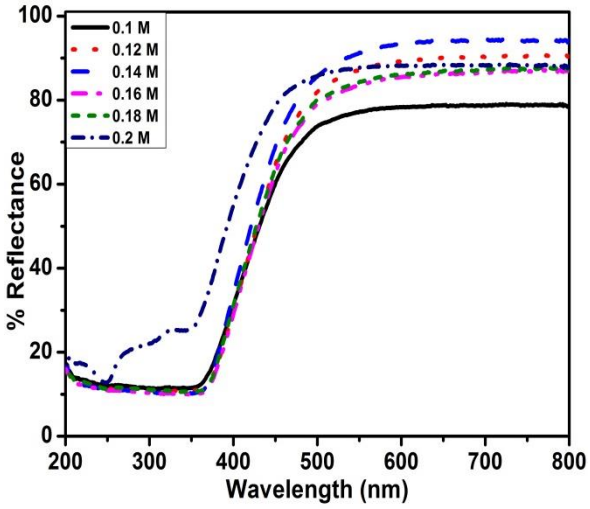

Figure 3. The comparison between diffuse reflectance curves of the ZnO prepared at different concentrations of ZnAc.

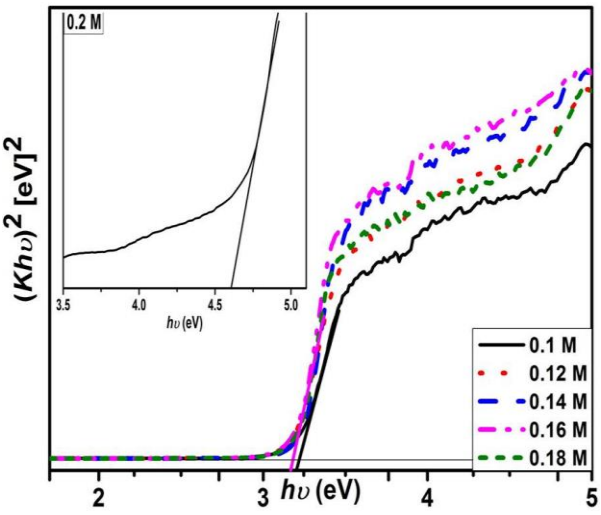

Figure 4. Estimate of the direct energy band gap of ZnO for different concentrations of ZnAc.

3.4. Photoluminescence analysis

Figure 5(a) shows the room temperature PL spectrum of the ZnO flower-like structure prepared at different concentrations of ZnAc. It can be seen that the emission spectrum consists of a broad band in the visible region with two main features. The PL spectrum for the sample prepared at the low ZnAc concentration of 0.1 M exhibits a dominant band emission in the blue region at ~ 450 nm, and a weak green band emission at ~ 528 nm. The luminescence band emission at ~ 450 nm is caused by the electronic transitions from zinc interstitial levels (Zn_i) to the valence band [17].The observed weak green emission at ~ 528 nm has been attributed by several authors to the oxygen vacancies (V_O) [18], therefore the green emission is due to radiative recombination of photo generated hole with an electron occupying the oxygen vacancy at the local level in the band gap [19]. It is clear that with increasing ZnAc concentration from 0.1 M to 0.18 M the blue emission is quenched while the green emission is enhanced (in proportion), and there is a small red-shift in the green emission. This phenomenon can be clearly seen in the inset in figure 5(a) wherein the spectrum for 0.2 M ZnAc is not included. Further increasing of the ZnAc concentration to 0.2 M enhanced the luminescence

intensity, indicating an increase in the density of defects such as zinc interstitial (Zn_i) and oxygen vacancies (V_O) within the ZnO nanoparticles.

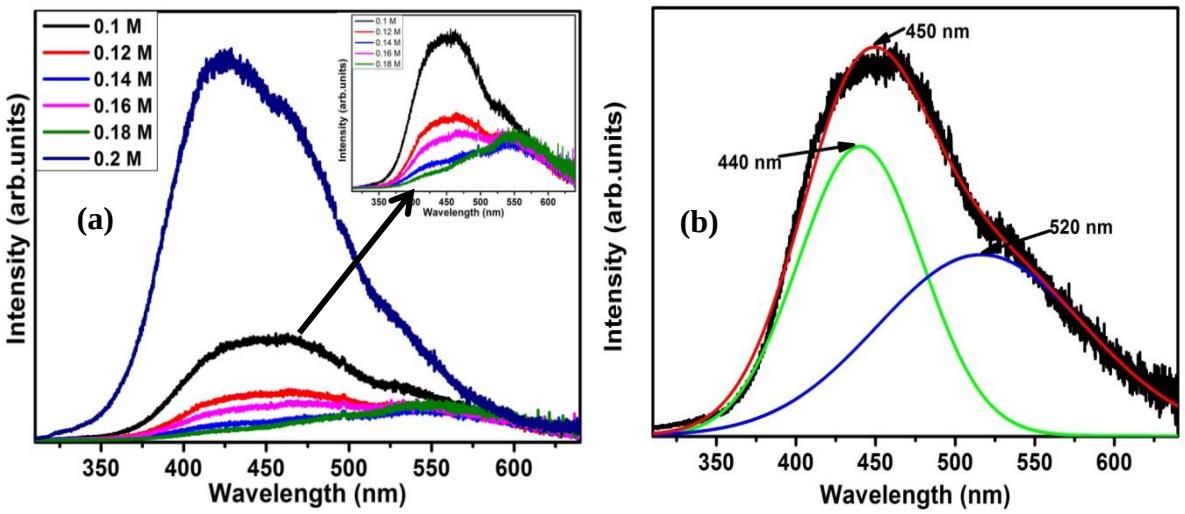

Figure 5. (a) Room temperature PL spectrum for ZnO flower-like structure prepared at different concentrations of ZnAc, (b) De-convoluted spectrum of ZnO sample prepared at 0.1 M ZnAc concentration.

Gaussian fits were only performed on the PL spectrum of ZnO prepared at 0.1 M ZnAc concentration as shown in figure 5(b). The de-convoluted spectrum shows two peaks centred at ~ 440, and ~ 520 nm. It is well known that a visible emission of zinc originates from intrinsic and structural defects [20]. The blue emission is observed at ~ 440 nm because of surface defects in ZnO, this emission is attributed to Zn interstitials (Zn_i) [21]. The weak green emission observed at ~ 520 nm is well attributed to singly ionized oxygen vacancy in ZnO [22]. The weak green emission at ~ 520 nm typically associated with the recombination of electrons trapped in singly ionized oxygen vacancy (V_o^+) with photo generated holes [23].

4. Conclusion

ZnO nanoparticles were successfully prepared using CBD method by varying molar concentrations of the ZnAc. There was no change in the crystallite size when increasing ZnAc concentration. Not uniform flower-like structure indicated that the morphology is independent from the ZnAc concentration. UV-vis spectroscopy shows no appreciable change in band gap energy of the flower-like structure when the ZnAc concentration increases. PL showed that the emission of the ZnO nanoparticles also depends on the ZnAc concentration.

Acknowledgements

Financial support for M.Sc in nanoscience from National Nanoscience Postgraduate Teaching and Training Programme (NNPTTP) program is highly acknowledged. The authors appreciate the extensive collaboration between UFS, UWC, NMMU and UJ.

References

[1] Kumar V, Swart H C, Ntwaeaborwa O M, Kroon R E, Terblans J J, Shaat S K K, Yousif A and Duvenhage M M 2013 *Mat. Lett*. **101** 57–60
[2] Abrarov S M, Yuldashev S U, Kim T W, Kwon Y H and Kang T W 2006 *Optics Commun.* **259** 378–384
[3] Sun X W, Huang J Z, Wang J X and Xu Z 2008 *Nano Lett.* **8** 1219–1223
[4] Meaney A J 2010 *On the growth and characterisation of Zinc Oxide* (Dublin City University,Glasnevin, Dublin 9, Ireland) p105
[5] Awodugba A O and Ilyas A O 2013 *Asian J. Appl. Sci.* **2** 41–44
[6] Sepet L, Baydogan N, Cimenoglu H, Kayali E S, Tugrul B, Altinsoy N, Albayrak G, Sengel H, Akmaz F and Parlar A 2011 *Def. Diff. Forum* **312–315** 836–841

[7] Wang Z L 2009 *Mat. Sci. Eng.* **64** 33–71
[8] Xu L, Guo Y, Liao Q, Zhang J and Xu D 2005 *J. Phys. Chem. B* **109** 13519–13522
[9] Kumar Vinod, Som S, Kumar Vijay, Kumar Vinay, Ntwaeaborwa O M, Coetsee E and Swart H C 2014 *Chem. Eng. J.* **255** 541–552
[10] Lu Y C, Wang L L, Xie T F, Chen L P and Lin Y H 2011 *Mater. Chem. Phys*. **129** 281–287
[11] Koao L F, Dejene F B and Swart H C 2014 *Mat. Sci. Sem. Proc*. **27** 33–40
[12] Cullity B D 1978 *Elements of X-ray Diffraction* (Addison-Wesley Publishing Company, Inc., London, 1978)
[13] Manzoor U and Kim D K 2009 *Physica E* **41** 500–505
[14] Polarz S, Roy A, Lehmann M, Driess M, Kruis F E, Hoffmann A and Zimmer P 2007 *Adv. Fun. Mater.* **17** 1385–1391
[15] Hu X, Masuda Y, Ohji T and Kato K 2010 *Key Eng. Mater.* **445** 123–126
[16] Molefe F V, Koao L F, Dolo J J and Dejene B F 2014 *Physica B*. **439** 185–188
[17] Motaung D E, Kortidis I, Papadaki D, Nkosi S S, Mhlongo G H, Wesley-Smith J, Malgas G F, Mwakikunga B W, Coetsee E, Swart H C, Kiriakidise G and Ray S S 2014 *App. Surf. Sci.* **311** 14–26
[18] Goswami N and Sharma D K 2010 *Physica E* **42** 1675–1682
[19] Mohanta A and Thareja R K 2008 *J. Appl. Phys*. **104** 044906
[20] Yim K G, Cho M Y, Jeon S M, Kim M S and Leem J Y 2011 *J. Korean Phys. Soc.* **58** 520–524
[21] Dutta S, and Ganguly B N 2012 *J Nanobiotech*. **10** 1–10
[22] Mazhdi M, Saydi J, Karimi M, Seidi J and Mazhdi F 2013 *Optik*. **124** 4128–4133
[23] Lin C Y, Wang W H, Lee C-S, Sun K W, and Suen Y W 2009 *Appl. Phys. Lett*. **94** 151909–151909-3